

15

Three-Node Plane Stress Triangles

TABLE OF CONTENTS

	Page
§15.1. Introduction	15-3
§15.2. Background	15-3
§15.2.1. Parametric Representation of Functions	15-3
§15.2.2. Geometry	15-4
§15.2.3. Triangular Coordinates	15-4
§15.2.4. Linear Interpolation	15-5
§15.2.5. Coordinate Transformations	15-5
§15.2.6. Partial Derivatives	15-6
§15.2.7. *Interesting Points and Lines	15-7
§15.3. The Turner Triangle	15-7
§15.3.1. Displacement Interpolation	15-8
§15.3.2. Strain-Displacement Equations	15-8
§15.3.3. Stress-Strain Equations	15-8
§15.3.4. The Stiffness Matrix	15-8
§15.3.5. The Consistent Nodal Force Vector	15-9
§15.3.6. Implementation	15-10
§15.3.7. *Consistency Verification	15-10
§15.3.8. *Checking Continuity	15-11
§15.3.9. *Checking Completeness	15-11
§15.3.10. *Tonti Matrix Diagram	15-12
§15.4. *Derivation Using Natural Strains and Stresses	15-12
§15.4.1. *Natural Strains and Stresses	15-12
§15.4.2. *Covariant Node Displacements	15-13
§15.4.3. *The Natural Stiffness Matrix	15-14
§15.5. *The Veubeke Equilibrium Triangle	15-14
§15.5.1. *Kinematic Relations	15-14
§15.5.2. *Stiffness Matrix	15-15
§15.5.3. *Implementation	15-15
§15.5.4. *Spurious Kinematic Modes	15-16
§15.6. *Shear Locking in Turner Triangles	15-17
§15.6.1. *The Inplane Bending Test	15-18
§15.6.2. *Energy Ratios	15-18
§15.6.3. *Convergence as Mesh is Refined	15-20
§15. Notes and Bibliography	15-20
§15. References	15-21
§15. Exercises	15-22

§15.1. Introduction

This Chapter derives element stiffness equations of three-node triangles constructed with linear displacements for the plane stress problem formulated in Chapter 14. These elements have six displacement degrees of freedom, which are placed at the *connection nodes*. There are two main versions that differ on where the connection nodes are located:

1. The *Turner triangle* has connection nodes located at the corners.
2. The *Veubeke equilibrium triangle* has connection nodes located at the side midpoints.

The triangle geometry is defined by the corner locations or *geometric nodes* in both cases. Of the two versions, the Turner triangle is by far the most practically important one in solid and structural mechanics.¹ Thus most of the material in this Chapter is devoted to it. It enjoys several important properties:

- (i) It belongs to both the isoparametric and subparametric element families, which are introduced in the next Chapter.
- (ii) It allows closed form derivations for the stiffness matrix and consistent force vector without need for numerical integration.
- (iii) It cannot be improved by the addition of internal degrees of freedom.

Properties (ii) and (iii) are shared by the Veubeke equilibrium triangle. Since this model is rarely used in structural applications it is covered only as advanced material in §15.5.

The Turner triangle is not a good performer for structural stress analysis. It is still used in problems that do not require high accuracy, as well as in non-structural applications such as thermal and electromagnetic analysis. One reason is that triangular meshes are easily generated over arbitrary two-dimensional domains using techniques such as Delaunay triangulation.

§15.2. Background

§15.2.1. Parametric Representation of Functions

The concept of *parametric representation* of functions is crucial in modern FEM. Together with multidimensional numerical integration, it is a key enabling tool for developing elements in two and three space dimensions.² Without these tools the developer would become lost in an algebraic maze as element geometry and shape functions get more complicated. The essentials of parametric representation can be illustrated through a simple example. Consider the following alternative representations of the unit-circle function, $x^2 + y^2 = 1$:

$$(I) \ y = \sqrt{1 - x^2}, \quad (II) \ x = \cos \theta \text{ and } y = \sin \theta. \quad (15.1)$$

The direct representation (I) fits the conventional function notation, i.e., $y = f(x)$. Given a value of x , it returns one or more y . On the other hand, the parametric representation (II) is indirect: both x

¹ The triangle was one of the two plane-stress continuum elements presented by Turner, Clough, Martin and Topp in their 1956 paper [254]. This publication is widely regarded as the start of the present FEM. The derivation was not done, however, with assumed displacements. See **Notes and Bibliography** at the end of this Chapter.

² Numerical integration is not useful for the triangular elements covered here, but essential in the more complicated iso-P models covered in Chapters 16ff.

and y are given in terms of one parameter, the angle θ . Elimination of θ through the trigonometric identity $\cos^2 \theta + \sin^2 \theta = 1$ recovers $x^2 + y^2 = 1$. But there are situations in which working with the parametric form throughout the development is more convenient. Continuum finite elements provide a striking illustration of this point.

§15.2.2. Geometry

The geometry of the 3-node triangle shown in Figure 15.1(a) is specified by the location of its three corner nodes on the $\{x, y\}$ plane. Nodes are labelled 1, 2, 3 while traversing the sides in *counterclockwise* fashion. Their location is defined by their Cartesian coordinates: $\{x_i, y_i\}$ for $i = 1, 2, 3$.

The Turner triangle has six degrees of freedom, defined by the six corner displacement components $\{u_{xi}, u_{yi}\}$, for $i = 1, 2, 3$. The interpolation of the internal displacements $\{u_x, u_y\}$ from these six values is studied in §15.3, after triangular coordinates are introduced. The triangle area can be obtained as

$$2A = \det \begin{bmatrix} 1 & 1 & 1 \\ x_1 & x_2 & x_3 \\ y_1 & y_2 & y_3 \end{bmatrix} = (x_2 y_3 - x_3 y_2) + (x_3 y_1 - x_1 y_3) + (x_1 y_2 - x_2 y_1). \quad (15.2)$$

The area given by (15.2) is a *signed* quantity. It is positive if the corners are numbered in cyclic counterclockwise order (when looking down from the $+z$ axis), as illustrated in Figure 15.1(b). This convention is followed in the sequel.

§15.2.3. Triangular Coordinates

Points of the triangle may also be located in terms of a *parametric* coordinate system:

$$\zeta_1, \zeta_2, \zeta_3. \quad (15.3)$$

In the literature these 3 parameters receive an astonishing number of names, as the list collected in Table 15.1 shows. In the sequel the name *triangular coordinates* will be used to emphasize the close association with this particular geometry.

Equations

$$\zeta_i = \text{constant} \quad (15.4)$$

represent a set of straight lines parallel to the side opposite to the i^{th} corner, as depicted in Figure 15.2. The equations of sides 2–3, 3–1 and 1–2 are $\zeta_1 = 0$, $\zeta_2 = 0$ and $\zeta_3 = 0$, respectively. The three corners have coordinates $(1,0,0)$, $(0,1,0)$ and $(0,0,1)$. The three midpoints of the sides have coordinates $(\frac{1}{2}, \frac{1}{2}, 0)$, $(0, \frac{1}{2}, \frac{1}{2})$ and $(\frac{1}{2}, 0, \frac{1}{2})$, the centroid has coordinates $(\frac{1}{3}, \frac{1}{3}, \frac{1}{3})$, and so on. The coordinates are not independent because their sum is unity:

$$\zeta_1 + \zeta_2 + \zeta_3 = 1. \quad (15.5)$$

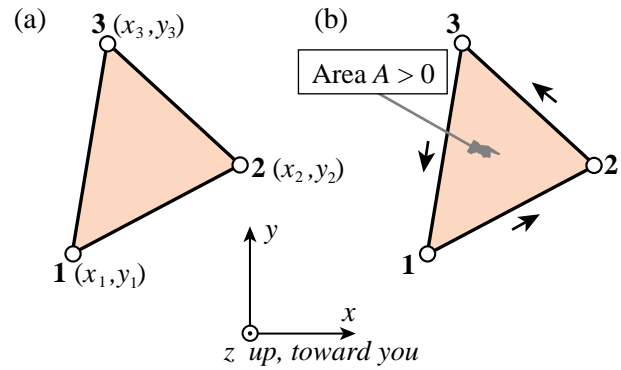
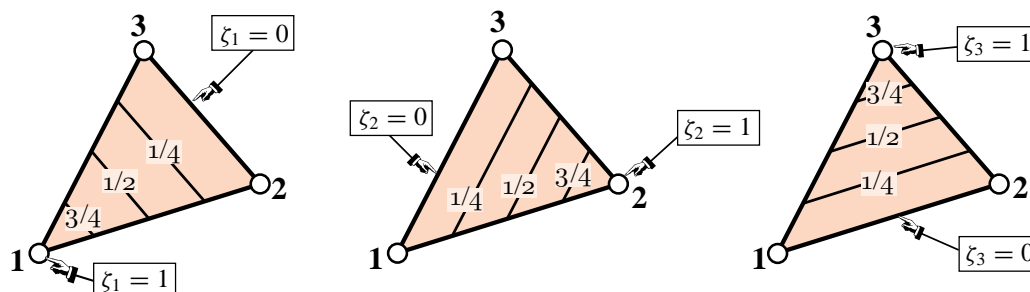


FIGURE 15.1. The three-node, linear-displacement plane stress triangular element: (a) geometry; (b) area and positive boundary traversal.

FIGURE 15.2. Triangular coordinates $\zeta_1, \zeta_2, \zeta_3$.**Table 15.1** Names of element parametric coordinates

<i>Name</i>	<i>Applicable to</i>
natural coordinates	all elements
isoparametric coordinates	isoparametric elements
shape function coordinates	isoparametric elements
barycentric coordinates	simplices (triangles, tetrahedra, ...)
Möbius coordinates	triangles
triangular coordinates	all triangles
area (also written “areal”) coordinates	straight-sided triangles
Triangular coordinates normalized as per $\zeta_1 + \zeta_2 + \zeta_3 = 1$ are often qualified as “homogeneous” in the mathematical literature.	

Remark 15.1. In pre-1970 FEM publications, triangular coordinates were often called *area coordinates*, and occasionally *areal coordinates*. This comes from the following interpretation: $\zeta_i = A_{jk}/A$, where A_{jk} is the area subtended by the subtriangle formed by the point P and corners j and k , in which j and k are 3-cyclic permutations of i . Historically this was the way coordinates were defined in 1960s papers. However this relation does not carry over to general isoparametric triangles with curved sides and thus it is not used here.

§15.2.4. Linear Interpolation

Consider a function $f(x, y)$ that varies *linearly* over the triangle domain. In terms of Cartesian coordinates it may be expressed as

$$f(x, y) = a_0 + a_1x + a_2y, \quad (15.6)$$

where a_0, a_1 and a_2 are coefficients to be determined from three conditions. In finite element work such conditions are often the *nodal values* taken by f at the corners:

$$f_1, f_2, f_3. \quad (15.7)$$

The expression in triangular coordinates makes direct use of those three values:

$$f(\zeta_1, \zeta_2, \zeta_3) = f_1\zeta_1 + f_2\zeta_2 + f_3\zeta_3 = [f_1 \ f_2 \ f_3] \begin{bmatrix} \zeta_1 \\ \zeta_2 \\ \zeta_3 \end{bmatrix} = [\zeta_1 \ \zeta_2 \ \zeta_3] \begin{bmatrix} f_1 \\ f_2 \\ f_3 \end{bmatrix}. \quad (15.8)$$

Formula (15.8) is called a *linear interpolant* for f .

§15.2.5. Coordinate Transformations

Quantities that are closely linked with the element geometry are best expressed in triangular coordinates. On the other hand, quantities such as displacements, strains and stresses are usually expressed in the Cartesian system $\{x, y\}$. Thus we need transformation equations through which it is possible to pass from one coordinate system to the other.

Cartesian and triangular coordinates are linked by the relation

$$\begin{bmatrix} 1 \\ x \\ y \end{bmatrix} = \begin{bmatrix} 1 & 1 & 1 \\ x_1 & x_2 & x_3 \\ y_1 & y_2 & y_3 \end{bmatrix} \begin{bmatrix} \zeta_1 \\ \zeta_2 \\ \zeta_3 \end{bmatrix}. \quad (15.9)$$

The first equation says that the sum of the three coordinates is one. The next two express x and y linearly as homogeneous forms in the triangular coordinates. These are obtained by applying the linear interpolant (15.8) to the Cartesian coordinates: $x = x_1\zeta_1 + x_2\zeta_2 + x_3\zeta_3$ and $y = y_1\zeta_1 + y_2\zeta_2 + y_3\zeta_3$. Assuming $A \neq 0$, inversion of (15.9) yields

$$\begin{bmatrix} \zeta_1 \\ \zeta_2 \\ \zeta_3 \end{bmatrix} = \frac{1}{2A} \begin{bmatrix} x_2y_3 - x_3y_2 & y_2 - y_3 & x_3 - x_2 \\ x_3y_1 - x_1y_3 & y_3 - y_1 & x_1 - x_3 \\ x_1y_2 - x_2y_1 & y_1 - y_2 & x_2 - x_1 \end{bmatrix} \begin{bmatrix} 1 \\ x \\ y \end{bmatrix} = \frac{1}{2A} \begin{bmatrix} 2A_{23} & y_{23} & x_{32} \\ 2A_{31} & y_{31} & x_{13} \\ 2A_{12} & y_{12} & x_{21} \end{bmatrix} \begin{bmatrix} 1 \\ x \\ y \end{bmatrix}. \quad (15.10)$$

Here $x_{jk} = x_j - x_k$, $y_{jk} = y_j - y_k$, A is the triangle area given by (15.2) and A_{jk} denotes the area subtended by corners j, k and the origin of the x - y system. If this origin is taken at the centroid of the triangle, $A_{23} = A_{31} = A_{12} = A/3$.

§15.2.6. Partial Derivatives

From equations (15.9) and (15.10) we immediately obtain the following relations between partial derivatives:

$$\frac{\partial x}{\partial \zeta_i} = x_i, \quad \frac{\partial y}{\partial \zeta_i} = y_i, \quad (15.11)$$

$$2A \frac{\partial \zeta_i}{\partial x} = y_{jk}, \quad 2A \frac{\partial \zeta_i}{\partial y} = x_{kj}. \quad (15.12)$$

In (15.12) j and k denote the 3-cyclic permutations of i . For example, if $i = 2$, then $j = 3$ and $k = 1$. The derivatives of a function $f(\zeta_1, \zeta_2, \zeta_3)$ with respect to x or y follow immediately from (15.12) and application of the chain rule:

$$\begin{bmatrix} \frac{\partial f}{\partial x} = \frac{1}{2A} \left(\frac{\partial f}{\partial \zeta_1} y_{23} + \frac{\partial f}{\partial \zeta_2} y_{31} + \frac{\partial f}{\partial \zeta_3} y_{12} \right) \\ \frac{\partial f}{\partial y} = \frac{1}{2A} \left(\frac{\partial f}{\partial \zeta_1} x_{32} + \frac{\partial f}{\partial \zeta_2} x_{13} + \frac{\partial f}{\partial \zeta_3} x_{21} \right) \end{bmatrix} \quad (15.13)$$

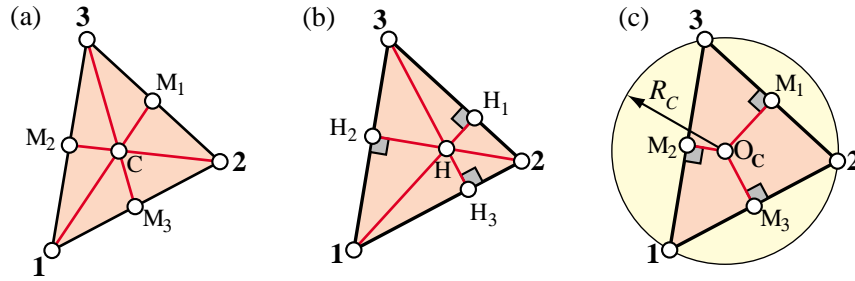


FIGURE 15.3. Interesting points and lines of a triangle.

which in matrix form is

$$\begin{bmatrix} \frac{\partial f}{\partial x} \\ \frac{\partial f}{\partial y} \end{bmatrix} = \frac{1}{2A} \begin{bmatrix} y_{23} & y_{31} & y_{12} \\ x_{32} & x_{13} & x_{21} \end{bmatrix} \begin{bmatrix} \frac{\partial f}{\partial \zeta_1} \\ \frac{\partial f}{\partial \zeta_2} \\ \frac{\partial f}{\partial \zeta_3} \end{bmatrix}. \quad (15.14)$$

With these mathematical ingredients in place we are now in a position to handle the derivation of straight-sided triangular elements, and in particular the Turner and Veubeke triangles.

§15.2.7. *Interesting Points and Lines

Some distinguished lines and points of a straight-sided triangle are briefly described here for use in other developments as well as in Exercises. The *triangle medians* are three lines that join the corners to the midpoints of the opposite sides, as pictured in Figure 15.3(a). The midpoint opposite corner i is labeled M_i .

The medians $1-M_1$, $2-M_2$ and $3-M_3$ have equations $\zeta_2 = \zeta_3$, $\zeta_3 = \zeta_1$ and $\zeta_1 = \zeta_2$, respectively, in triangular coordinates. They intersect at the centroid C of coordinates $\{\frac{1}{3}, \frac{1}{3}, \frac{1}{3}\}$. Other names for the centroid are *barycenter* and *center of gravity*. If you make a real triangle out of cardboard, you can balance the triangle at this point. It can be shown that the centroid trisects the medians, that is to say, the distance from a corner to the centroid is twice the distance from the centroid to the opposite side of the triangle.

The *altitudes* are three lines that connect each corner with their projections onto the opposing sides, as depicted in Figure 15.3(b). The projection of corner i is identified H_i , so the altitudes are $1-H_1$, $2-H_2$ and $3-H_3$. Locations H_i are called *altitude feets*. The altitudes intersect at the triangle *orthocenter* H . The lengths of those segments are the *triangle heights*. The triangular coordinates of H_i and H , as well as the altitude equations, are worked out in an Exercise.

Another interesting point is the center O_C of the circumscribed circle, or circumcircle. This is the unique circle that passes through the three corners, as shown in Figure 15.3(c). It can be geometrically constructed by drawing the normal to each side at the midpoints. Those three lines, called the perpendicular side bisectors, intersect at O_C . A famous theorem by Euler asserts that the centroid, the orthocenter and the circumcircle center fall on a straight line, called the Euler line. Furthermore, C lies between O_C and H , and the distance O_C-H is three times the distance $H-C$.

§15.3. The Turner Triangle

The simplest triangular element for plane stress (and in general, for 2D problems of variational index $m = 1$) is the three-node triangle with *linear shape functions*, with degrees of freedom

located at the corners. The shape functions are simply the triangular coordinates. That is, $N_i^e = \zeta_i$ for $i = 1, 2, 3$. When applied to the plane stress problem, this element is called the Turner triangle.

§15.3.1. Displacement Interpolation

For the plane stress problem we select the linear interpolation (15.8) for the displacement components u_x and u_y at an arbitrary point $P(\zeta_1, \zeta_2, \zeta_3)$:

$$u_x = u_{x1}\zeta_1 + u_{x2}\zeta_2 + u_{x3}\zeta_3, \quad u_y = u_{y1}\zeta_1 + u_{y2}\zeta_2 + u_{y3}\zeta_3. \quad (15.15)$$

The interpolation is illustrated in Figure 15.4. The two expressions in (15.15) can be combined in a matrix form that befits the expression (14.17) for an arbitrary plane stress element:

$$\begin{bmatrix} u_x \\ u_y \end{bmatrix} = \begin{bmatrix} \zeta_1 & 0 & \zeta_2 & 0 & \zeta_3 & 0 \\ 0 & \zeta_1 & 0 & \zeta_2 & 0 & \zeta_3 \end{bmatrix} \begin{bmatrix} u_{x1} \\ u_{y1} \\ u_{x2} \\ u_{y2} \\ u_{x3} \\ u_{y3} \end{bmatrix} = \mathbf{N} \mathbf{u}^e, \quad (15.16)$$

where \mathbf{N} is the matrix of shape functions.

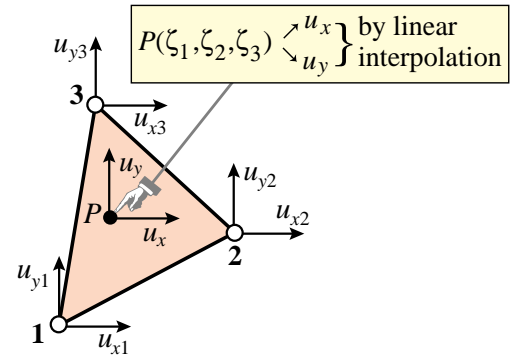


FIGURE 15.4. Displacement interpolation over triangle.

§15.3.2. Strain-Displacement Equations

The strains within the elements are obtained by differentiating the shape functions with respect to x and y . Using (15.14), (15.16) and the general form (14.18) we get

$$\mathbf{e} = \mathbf{D} \mathbf{N} \mathbf{u}^e = \frac{1}{2A} \begin{bmatrix} y_{23} & 0 & y_{31} & 0 & y_{12} & 0 \\ 0 & x_{32} & 0 & x_{13} & 0 & x_{21} \\ x_{32} & y_{23} & x_{13} & y_{31} & x_{21} & y_{12} \end{bmatrix} \begin{bmatrix} u_{x1} \\ u_{y1} \\ u_{x2} \\ u_{y2} \\ u_{x3} \\ u_{y3} \end{bmatrix} = \mathbf{B} \mathbf{u}^e, \quad (15.17)$$

in which \mathbf{D} denotes the symbolic strain-to-displacement differentiation operator given in (14.6), and \mathbf{B} is the strain-displacement matrix. Note that the strains are *constant* over the element. This is the origin of the name *constant strain triangle* (CST) given it in many finite element publications.

§15.3.3. Stress-Strain Equations

The stress field $\boldsymbol{\sigma}$ is related to the strain field by the elastic constitutive equation in (14.5), which is repeated here for convenience:

$$\boldsymbol{\sigma} = \begin{bmatrix} \sigma_{xx} \\ \sigma_{yy} \\ \sigma_{xy} \end{bmatrix} = \begin{bmatrix} E_{11} & E_{12} & E_{13} \\ E_{12} & E_{22} & E_{23} \\ E_{13} & E_{23} & E_{33} \end{bmatrix} \begin{bmatrix} e_{xx} \\ e_{yy} \\ 2e_{xy} \end{bmatrix} = \mathbf{E} \mathbf{e}, \quad (15.18)$$

where E_{ij} are plane stress elastic moduli. The constitutive matrix \mathbf{E} will be assumed to be constant over the element. Because the strains are constant, so are the stresses.

§15.3.4. The Stiffness Matrix

The element stiffness matrix is given by the general formula (14.23), which is repeated here

$$\mathbf{K}^e = \int_{\Omega^e} h \mathbf{B}^T \mathbf{E} \mathbf{B} d\Omega, \quad (15.19)$$

where Ω^e is the triangle domain, and h the plate thickness that appears in the plane stress problem. Since \mathbf{B} and \mathbf{E} are constant, they can be taken out of the integral:

$$\mathbf{K}^e = \mathbf{B}^T \mathbf{E} \mathbf{B} \int_{\Omega^e} h d\Omega \quad (15.20)$$

If h is uniform over the element the remaining integral in (15.20) is simply hA , and we obtain the closed form

$$\mathbf{K}^e = A h \mathbf{B}^T \mathbf{E} \mathbf{B} = \frac{h}{4A} \begin{bmatrix} y_{23} & 0 & x_{32} \\ 0 & x_{32} & y_{23} \\ y_{31} & 0 & x_{13} \\ 0 & x_{13} & y_{31} \\ y_{12} & 0 & x_{21} \\ 0 & x_{21} & y_{12} \end{bmatrix} \begin{bmatrix} E_{11} & E_{12} & E_{13} \\ E_{12} & E_{22} & E_{23} \\ E_{13} & E_{23} & E_{33} \end{bmatrix} \begin{bmatrix} y_{23} & 0 & y_{31} & 0 & y_{12} & 0 \\ 0 & x_{32} & 0 & x_{13} & 0 & x_{21} \\ x_{32} & y_{23} & x_{13} & y_{31} & x_{21} & y_{12} \end{bmatrix}. \quad (15.21)$$

Exercise 15.1 deals with the case of a linearly varying plate thickness.

§15.3.5. The Consistent Nodal Force Vector

For simplicity we consider here only internal body forces³ defined by the vector field

$$\mathbf{b} = \begin{bmatrix} b_x \\ b_y \end{bmatrix} \quad (15.22)$$

which is specified per unit of volume. The consistent nodal force vector \mathbf{f}^e is given by the general formula (14.23) of the previous Chapter:

$$\mathbf{f}^e = \int_{\Omega^e} h \mathbf{N}^T \mathbf{b} d\Omega = \int_{\Omega^e} h \begin{bmatrix} \zeta_1 & 0 \\ 0 & \zeta_1 \\ \zeta_2 & 0 \\ 0 & \zeta_2 \\ \zeta_3 & 0 \\ 0 & \zeta_3 \end{bmatrix} \mathbf{b} d\Omega. \quad (15.23)$$

The simplest case is when the body force components (15.22) as well as the thickness h are constant over the element. Then we need the integrals

$$\int_{\Omega^e} \zeta_1 d\Omega = \int_{\Omega^e} \zeta_2 d\Omega = \int_{\Omega^e} \zeta_3 d\Omega = \frac{1}{3}A \quad (15.24)$$

³ For consistent force computations corresponding to distributed boundary loads over a side, see Exercise 15.4.

```

Trig3TurnerMembraneStiffness[ncoor_,Emat_,h_,numer_] := Module[{
  x1,x2,x3,y1,y2,y3,x21,x32,x13,y12,y23,y31,A,Be,Ke},
  {{x1,y1},{x2,y2},{x3,y3}} = ncoor;
  A = Simplify[(x2*y3-x3*y2+(x3*y1-x1*y3)+(x1*y2-x2*y1))/2];
  {x21,x32,x13,y12,y23,y31} = {x2-x1,x3-x2,x1-x3,y1-y2,y2-y3,y3-y1};
  Be = {{y23,0,y31,0,y12,0},{0,x32,0,x13,0,x21},
        {x32,y23,x13,y31,x21,y12}}/(2*A);
  If[numer, Be = N[Be]]; Ke = A*h*Transpose[Be].Emat.Be;
  Return[Ke];

```

FIGURE 15.5. Implementation of Turner triangle stiffness matrix calculation as a *Mathematica* module.

which replaced into (15.23) gives

$$\mathbf{f}^e = \frac{Ah}{3} [b_x \quad b_y \quad b_x \quad b_y \quad b_x \quad b_y]^T. \quad (15.25)$$

This agrees with the simple element-by-element force-lumping procedure, which assigns one third of the total force along the $\{x, y\}$ directions: Ahb_x and Ahb_y , to each corner.

Remark 15.2. The integrals (15.24) are particular cases of the general integration formula of monomials in triangular coordinates:

$$\frac{1}{2A} \int_{\Omega^e} \xi_1^i \xi_2^j \xi_3^k d\Omega = \frac{i!j!k!}{(i+j+k+2)!}, \quad i \geq 0, j \geq 0, k \geq 0. \quad (15.26)$$

which can be derived through the Beta function. Here i, j, k are integer exponents. This formula *only holds for triangles with straight sides*, and thus does not apply for higher order elements with curved sides. Formulas (15.24) are obtained by setting exponents $i = 1, j = k = 0$ in (15.26), and permuting $\{i, j, k\}$ cyclically.

§15.3.6. Implementation

The implementation of the Turner triangle in any programming language is very simple. A *Mathematica* module that returns \mathbf{K}^e is shown in Figure 15.5. The module needs only 8 lines of code. It is invoked as

$$\mathbf{K}^e = \text{Trig3TurnerMembraneStiffness}[\text{ncoor}, \text{Emat}, h, \text{numer}]; \quad (15.27)$$

The arguments are

ncoor	Element node coordinates, arranged as a list: $\{\{x_1, y_1\}, \{x_2, y_2\}, \{x_3, y_3\}\}$.
Emat	A two-dimensional list storing the 3×3 plane stress matrix of elastic moduli as $\{\{E_{11}, E_{12}, E_{13}\}, \{E_{12}, E_{22}, E_{23}\}, \{E_{13}, E_{23}, E_{33}\}\}$.
h	Plate thickness, assumed uniform over the triangle.
numer	A logical flag: True to request floating-point computation, else False.

This module is exercised by the statements listed at the top of Figure 15.6, which form a triangle with corner coordinates $\{\{0, 0\}, \{3, 1\}, \{2, 2\}\}$, isotropic material matrix with $E_{11} = E_{22} = 64$, $E_{12} = 16$, $E_{33} = 24$, others zero, (that is, $E = 60$ and $\nu = \frac{1}{4}$) and unit thickness. The results are shown at the bottom of Figure 15.6. The computation of stiffness matrix eigenvalues is always a good programming test, since 3 eigenvalues must be exactly zero and the other 3 real and positive, as explained in Chapter 19. The last test statement draws the triangle (this plot was moved to the right of the numeric output to save space.)

```

ncoor={{0,0},{3,1},{2,2}}; Emat=8*{{8,2,0},{2,8,0},{0,0,3}};
Ke=Trig3TurnerMembraneStiffness[ncoor,Emat,1,False];
Print["Ke=",Ke//MatrixForm];
Print["eigs of Ke=",Chop[Eigenvalues[N[Ke]]]];
Show[Graphics[RGBColor[1,0,0]],Graphics[AbsoluteThickness[2]],
Graphics[Polygon[ncoor]],Axes->True];

```

$$Ke = \begin{pmatrix} 11 & 5 & -10 & -2 & -1 & -3 \\ 5 & 11 & 2 & 10 & -7 & -21 \\ -10 & 2 & 44 & -20 & -34 & 18 \\ -2 & 10 & -20 & 44 & 22 & -54 \\ -1 & -7 & -34 & 22 & 35 & -15 \\ -3 & -21 & 18 & -54 & -15 & 75 \end{pmatrix}$$

eigs of Ke = {139.33, 60., 20.6704, 0, 0, 0}

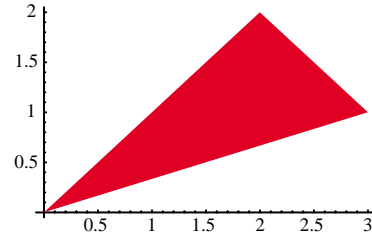


FIGURE 15.6. Test statements to exercise the module of Figure 15.5, and outputs.

§15.3.7. *Consistency Verification

It remains to check whether the interpolation (15.15) for element displacements meets the completeness and continuity criteria studied in Chapter 19 for finite element trial functions. Such *consistency* conditions are sufficient to insure convergence toward the exact solution of the mathematical model as the mesh is refined.

The variational index for the plane stress problem is $m = 1$. According to the rules stated in §19.3, the trial functions should be 1-complete, C^0 continuous, and C^1 piecewise differentiable.

§15.3.8. *Checking Continuity

Along any triangle side, the variation of u_x and u_y is *linear and uniquely determined by the value at the nodes on that side*. For example, over side 1-2 of an individual triangle, which has equation $\zeta_3 = 0$:

$$\begin{aligned} u_x &= u_{x1}\zeta_1 + u_{x2}\zeta_2 + u_{x3}\zeta_3 = u_{x1}\zeta_1 + u_{x2}\zeta_2, \\ u_y &= u_{y1}\zeta_1 + u_{y2}\zeta_2 + u_{y3}\zeta_3 = u_{y1}\zeta_1 + u_{y2}\zeta_2. \end{aligned} \quad (15.28)$$

An identical argument holds for that side when it belongs to an adjacent triangle, such as elements (e1) and (e2) shown in Figure 15.7. Since the node values on all elements that meet at a node are the same, u_x and u_y match along the side, and the trial function is C^0 interelement continuous. Because the functions are continuous inside the elements, it follows that the continuity requirement is met.

The variation of u_x and u_y over side 1-2 depends only on the nodal values u_{x1}, u_{x2}, u_{y1} and u_{y2} .

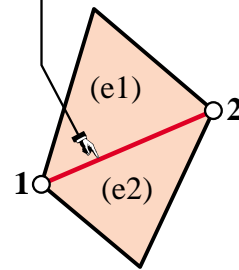


FIGURE 15.7. Interelement continuity check.

§15.3.9. *Checking Completeness

The completeness condition for variational order $m = 1$ requires that the shape functions $N_i = \zeta_i$ be able to represent exactly any linear displacement field:

$$u_x = \alpha_0 + \alpha_1 x + \alpha_2 y, \quad u_y = \beta_0 + \beta_1 x + \beta_2 y. \quad (15.29)$$

To check this we obtain the nodal values associated with the motion (15.29): $u_{xi} = \alpha_0 + \alpha_1 x_i + \alpha_2 y_i$ and $u_{yi} = \beta_0 + \beta_1 x_i + \beta_2 y_i$ for $i = 1, 2, 3$. Replace these in (15.16) and see if (15.29) is recovered. Here are the detailed calculations for component u_x :

$$\begin{aligned} u_x &= \sum_i u_{xi} \zeta_i = \sum_i (\alpha_0 + \alpha_1 x_i + \alpha_2 y_i) \zeta_i = \sum_i (\alpha_0 \zeta_i + \alpha_1 x_i \zeta_i + \alpha_2 y_i \zeta_i) \\ &= \alpha_0 \sum_i \zeta_i + \alpha_1 \sum_i (x_i \zeta_i) + \alpha_2 \sum_i (y_i \zeta_i) = \alpha_0 + \alpha_1 x + \alpha_2 y. \end{aligned} \quad (15.30)$$

Component u_y can be similarly verified. Consequently (15.16) satisfies the completeness requirement for the plane stress problem — and in general, for any problem of variational index 1. Finally, a piecewise linear trial function is obviously C^1 piecewise differentiable and consequently has finite energy. Thus the two completeness requirements are satisfied.

§15.3.10. *Tonti Matrix Diagram

For further developments covered in more advanced courses, it is convenient to split the governing equations of the element. In the case of the Turner triangle they are, omitting element superscripts:

$$\mathbf{e} = \mathbf{B}\mathbf{u}, \quad \boldsymbol{\sigma} = \mathbf{E}\mathbf{e}, \quad \mathbf{f} = \mathbf{A}^T \boldsymbol{\sigma} = V \mathbf{B}^T \boldsymbol{\sigma}. \quad (15.31)$$

Here $V = h_m A$ is the volume of the element, h_m being the mean thickness. The equations (15.31) may be graphically represented with the diagram shown in Figure 15.8. This is a discrete Tonti diagram similar to those of Chapter 6.

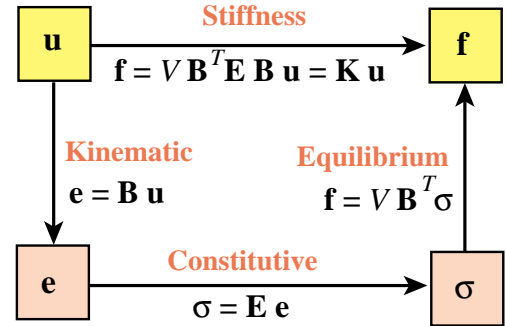


FIGURE 15.8. Tonti matrix diagram for Turner triangle.

§15.4. *Derivation Using Natural Strains and Stresses

The foregoing derivation of the Turner triangle uses Cartesian strains and stresses, as well as $\{x, y\}$ displacements. The only intrinsic quantities are the triangle coordinates. This advanced section examines the derivation of the element stiffness matrix through natural strains, natural stresses and covariant displacements.

Although the procedure does not offer obvious shortcuts over the previous derivation, it becomes important in the construction of more complicated high performance elements. It also helps reading recent literature in assumed strain elements.

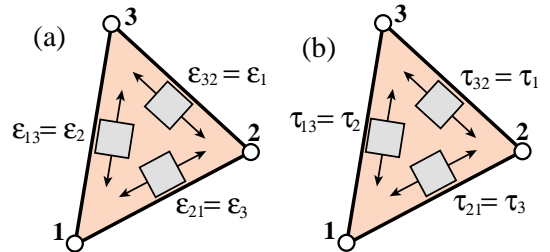


FIGURE 15.9. Geometry-intrinsic fields for the Turner triangle: (a) natural strains ϵ_i , (b) natural stresses τ_i .

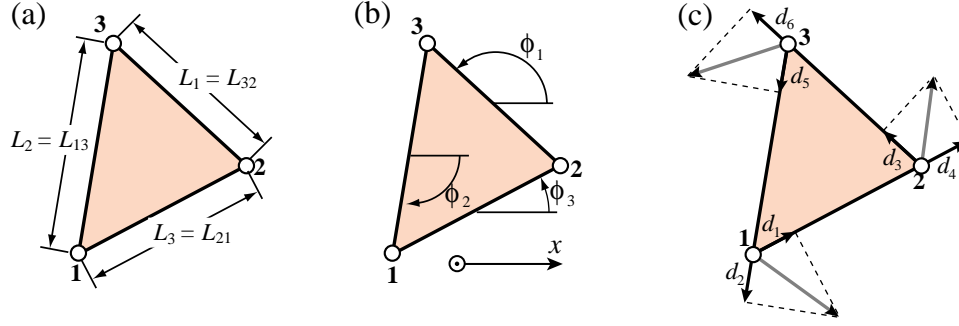


FIGURE 15.10. Additional quantities appearing in natural strain and stress calculations: (a) side lengths, (b) side directions, (c) covariant node displacements.

§15.4.1. *Natural Strains and Stresses

Natural strains are extensional strains directed parallel to the triangle sides, as shown in Figure 15.9(a). Natural strains are denoted by $\epsilon_{21} \equiv \epsilon_3$, $\epsilon_{32} \equiv \epsilon_1$, and $\epsilon_{13} \equiv \epsilon_2$.

Similarly, *natural stresses* are normal stresses directed parallel to the triangle sides, as shown in Figure 15.9(b). Natural stresses are denoted by $\tau_{21} \equiv \tau_3$, $\tau_{32} \equiv \tau_1$, and $\tau_{13} \equiv \tau_2$.

Because both natural stresses and strains are constant over the triangle, no node value association is needed.

The natural strains can be related to Cartesian strains by the following tensor transformation⁴

$$\boldsymbol{\epsilon} = \begin{bmatrix} \epsilon_1 \\ \epsilon_2 \\ \epsilon_3 \end{bmatrix} = \begin{bmatrix} c_1^2 & s_1^2 & s_1 c_1 \\ c_2^2 & s_2^2 & s_2 c_2 \\ c_3^2 & s_3^2 & s_3 c_3 \end{bmatrix} \begin{bmatrix} e_{xx} \\ e_{yy} \\ 2e_{xy} \end{bmatrix} = \mathbf{T}_e^{-1} \mathbf{e}. \quad (15.32)$$

Here $c_1 = x_{32}/L_1$, $s_1 = y_{32}/L_1$, $c_2 = x_{13}/L_2$, $s_2 = y_{13}/L_2$, $c_3 = x_{21}/L_3$, and $s_3 = y_{21}/L_3$, are sines and cosines of the side directions with respect to $\{x, y\}$, as illustrated in Figure 15.10(a,b). The inverse of this relation is

$$\mathbf{e} = \begin{bmatrix} e_{xx} \\ e_{yy} \\ 2e_{xy} \end{bmatrix} = \frac{1}{4A^2} \begin{bmatrix} y_{31}y_{21}L_1^2 & y_{12}y_{32}L_2^2 & y_{23}y_{13}L_3^2 \\ x_{31}x_{21}L_1^2 & x_{12}x_{32}L_2^2 & x_{23}x_{13}L_3^2 \\ (y_{31}x_{12} + x_{13}y_{21})L_1^2 & (y_{12}x_{23} + x_{21}y_{32})L_2^2 & (y_{23}x_{31} + x_{32}y_{13})L_3^2 \end{bmatrix} \begin{bmatrix} \epsilon_1 \\ \epsilon_2 \\ \epsilon_3 \end{bmatrix} = \mathbf{T}_e \boldsymbol{\epsilon}. \quad (15.33)$$

Note that \mathbf{T}_e is constant over the triangle. From the invariance of the strain energy density $\boldsymbol{\sigma}^T \mathbf{e} = \boldsymbol{\tau}^T \boldsymbol{\epsilon}$ it follows that the stresses transform as $\boldsymbol{\tau} = \mathbf{T}_e \boldsymbol{\sigma}$ and $\boldsymbol{\sigma} = \mathbf{T}_e^{-1} \boldsymbol{\tau}$. That strain energy density may be expressed as

$$\mathcal{U} = \frac{1}{2} \mathbf{e}^T \mathbf{E} \mathbf{e} = \frac{1}{2} \boldsymbol{\epsilon}^T \mathbf{E}_n \boldsymbol{\epsilon}, \quad \mathbf{E}_n = \mathbf{T}_e^T \mathbf{E} \mathbf{T}_e. \quad (15.34)$$

Here \mathbf{E}_n is a stress-strain matrix that relates natural stresses to natural strains as $\boldsymbol{\tau} = \mathbf{E}_n \boldsymbol{\epsilon}$. It may be therefore called the natural constitutive matrix.

§15.4.2. *Covariant Node Displacements

Covariant node displacements d_i are directed along the side directions, as shown in Figure 15.10(c), which

⁴ This is the “straingage rosette” transformation studied in Mechanics of Materials books.

defines the notation used for them. They are related to the Cartesian node displacements by

$$\mathbf{d} = \begin{bmatrix} d_1 \\ d_2 \\ d_3 \\ d_4 \\ d_5 \\ d_6 \end{bmatrix} = \begin{bmatrix} c_3 & s_3 & 0 & 0 & 0 & 0 \\ c_2 & s_2 & 0 & 0 & 0 & 0 \\ 0 & 0 & c_1 & s_1 & 0 & 0 \\ 0 & 0 & c_3 & s_3 & 0 & 0 \\ 0 & 0 & 0 & 0 & c_2 & s_2 \\ 0 & 0 & 0 & 0 & c_1 & s_1 \end{bmatrix} \begin{bmatrix} u_{x1} \\ u_{y1} \\ u_{x2} \\ u_{y2} \\ u_{x3} \\ u_{y3} \end{bmatrix} = \mathbf{T}_d \mathbf{u}. \quad (15.35)$$

The inverse relation is

$$\mathbf{u} = \begin{bmatrix} u_{x1} \\ u_{y1} \\ u_{x2} \\ u_{y2} \\ u_{x3} \\ u_{y3} \end{bmatrix} = \frac{1}{2A} \begin{bmatrix} L_3 y_{31} & L_2 y_{21} & 0 & 0 & 0 & 0 \\ L_3 x_{13} & L_2 x_{12} & 0 & 0 & 0 & 0 \\ 0 & 0 & L_1 y_{12} & L_3 y_{32} & 0 & 0 \\ 0 & 0 & L_1 x_{21} & L_3 x_{23} & 0 & 0 \\ 0 & 0 & 0 & 0 & L_2 y_{23} & L_1 y_{13} \\ 0 & 0 & 0 & 0 & L_2 x_{32} & L_1 x_{31} \end{bmatrix} \begin{bmatrix} d_1 \\ d_2 \\ d_3 \\ d_4 \\ d_5 \\ d_6 \end{bmatrix} = \mathbf{T}_d^{-1} \mathbf{d}. \quad (15.36)$$

The natural strains are evidently given by the relations $\epsilon_1 = (d_6 - d_3)/L_1$, $\epsilon_2 = (d_2 - d_5)/L_2$ and $\epsilon_3 = (d_4 - d_1)/L_3$. Collecting these in matrix form:

$$\boldsymbol{\epsilon} = \begin{bmatrix} \epsilon_1 \\ \epsilon_2 \\ \epsilon_3 \end{bmatrix} = \begin{bmatrix} 0 & 0 & -1/L_1 & 0 & 0 & 1/L_1 \\ 0 & 1/L_2 & 0 & 0 & -1/L_2 & 0 \\ -1/L_3 & 0 & 0 & 1/L_3 & 0 & 0 \end{bmatrix} \begin{bmatrix} d_1 \\ d_2 \\ d_3 \\ d_4 \\ d_5 \\ d_6 \end{bmatrix} = \mathbf{B}_\epsilon \mathbf{d}. \quad (15.37)$$

§15.4.3. *The Natural Stiffness Matrix

The natural stiffness matrix for constant thickness h is

$$\mathbf{K}_n^e = (Ah) \mathbf{B}_\epsilon^T \mathbf{E}_n \mathbf{B}_\epsilon, \quad \mathbf{E}_n = \mathbf{T}_e^T \mathbf{E} \mathbf{T}_e. \quad (15.38)$$

The Cartesian stiffness matrix is

$$\mathbf{K}^e = \mathbf{T}_d^T \mathbf{K}_n \mathbf{T}_d. \quad (15.39)$$

Comparing with $\mathbf{K}^e = (Ah) \mathbf{B}^T \mathbf{E} \mathbf{B}$ we see that

$$\mathbf{B} = \mathbf{T}_e \mathbf{B}_\epsilon \mathbf{T}_d, \quad \mathbf{B}_\epsilon = \mathbf{T}_e^{-1} \mathbf{B} \mathbf{T}_d^{-1}. \quad (15.40)$$

§15.5. *The Veubeke Equilibrium Triangle

The Veubeke equilibrium triangle⁵ differs from the Turner triangle in the degree-of-freedom configuration. As illustrated in Figure 15.11, those are moved to the midpoints {4, 5, 6} while the corner nodes {1, 2, 3} still define the geometry of the element. In the FEM terminology introduced in Chapter 6, the geometric nodes {1, 2, 3} and the connection nodes {4, 5, 6} no longer coincide. The node displacement vector collects the freedoms shown in Figure 15.11(b):

$$\mathbf{u}^e = [u_{x4} \quad u_{y4} \quad u_{x5} \quad u_{y5} \quad u_{x6} \quad u_{y6}]^T. \quad (15.41)$$

The quickest way to formulate the stiffness matrix of this element is to relate (15.41) to the node displacements of the Turner triangle, renamed for convenience as

$$\mathbf{u}_T^e = [u_{x1} \quad u_{y1} \quad u_{x2} \quad u_{y2} \quad u_{x3} \quad u_{y3}]^T. \quad (15.42)$$

⁵ The qualifier *equilibrium* distinguishes this element from others created by Fraeijs de Veubeke, including the 6-node plane stress conforming triangle. See **Notes and Bibliography** for the original derivation from an equilibrium field.

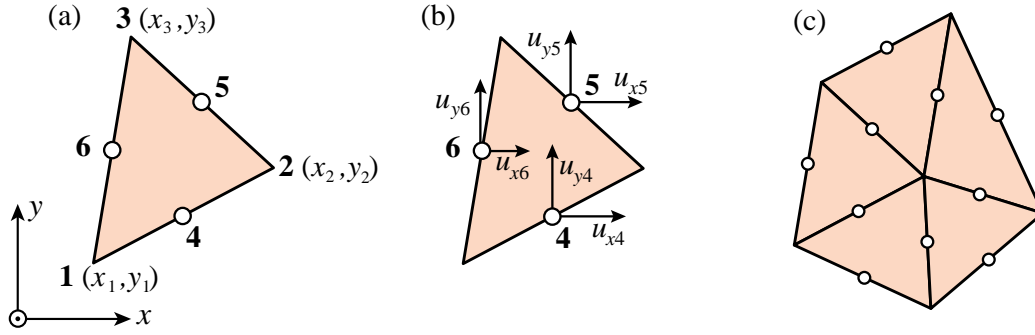


FIGURE 15.11. The Veubeke equilibrium triangle: (a) geometric definition; (b) degree-of-freedom configuration; (c) element patch showing how triangles are connected at the midpoints.

§15.5.1. *Kinematic Relations

The node freedom vectors (15.41) and (15.42) are easily related since by linear interpolation along the sides one obviously has $u_{x4} = \frac{1}{2}(u_{x1} + u_{x2})$, $u_{y4} = \frac{1}{2}(u_{y1} + u_{y2})$, etc. Expressing those links in matrix form gives

$$\begin{bmatrix} u_{x4} \\ u_{y4} \\ u_{x5} \\ u_{y5} \\ u_{x6} \\ u_{y6} \end{bmatrix} = \frac{1}{2} \begin{bmatrix} 1 & 0 & 1 & 0 & 0 & 0 \\ 0 & 1 & 0 & 1 & 0 & 0 \\ 0 & 0 & 1 & 0 & 1 & 0 \\ 0 & 0 & 0 & 1 & 0 & 1 \\ 1 & 0 & 0 & 0 & 1 & 0 \\ 0 & 1 & 0 & 0 & 0 & 1 \end{bmatrix} \begin{bmatrix} u_{x1} \\ u_{y1} \\ u_{x2} \\ u_{y2} \\ u_{x3} \\ u_{y3} \end{bmatrix}, \quad \begin{bmatrix} u_{x1} \\ u_{y1} \\ u_{x2} \\ u_{y2} \\ u_{x3} \\ u_{y3} \end{bmatrix} = \begin{bmatrix} 1 & 0 & -1 & 0 & 1 & 0 \\ 0 & 1 & 0 & -1 & 0 & 1 \\ 1 & 0 & 1 & 0 & -1 & 0 \\ 0 & 1 & 0 & 1 & 0 & -1 \\ -1 & 0 & 1 & 0 & 1 & 0 \\ 0 & -1 & 0 & 1 & 0 & 1 \end{bmatrix} \begin{bmatrix} u_{x4} \\ u_{y4} \\ u_{x5} \\ u_{y5} \\ u_{x6} \\ u_{y6} \end{bmatrix}. \quad (15.43)$$

In compact form: $\mathbf{u}^e = \mathbf{T}_{VT} \mathbf{u}_T^e$ and $\mathbf{u}_T^e = \mathbf{T}_{TV} \mathbf{u}^e$, with $\mathbf{T}_{VT} = \mathbf{T}_{TV}^{-1}$. The shape functions are

$$N_4 = \zeta_1 + \zeta_2 - \zeta_3, \quad N_5 = -\zeta_1 + \zeta_2 + \zeta_3, \quad N_6 = \zeta_1 - \zeta_2 + \zeta_3. \quad (15.44)$$

Renaming the Turner triangle strain-displacement matrix of (15.17) as \mathbf{B}_T , the corresponding matrix that relates $\mathbf{e} = \mathbf{B} \mathbf{u}^e$ in the Veubeke equilibrium triangle becomes

$$\mathbf{B} = \mathbf{B}_T \mathbf{T}_{TV} = \frac{1}{A} \begin{bmatrix} y_{21} & 0 & y_{32} & 0 & y_{13} & 0 \\ 0 & x_{12} & 0 & x_{23} & 0 & x_{31} \\ x_{12} & y_{21} & x_{23} & y_{32} & x_{31} & y_{13} \end{bmatrix} \quad (15.45)$$

§15.5.2. *Stiffness Matrix

The element stiffness matrix is given by the general formula (14.23). For constant plate thickness h one obtains the closed form

$$\mathbf{K}^e = A h \mathbf{B}^T \mathbf{E} \mathbf{B} = \frac{h}{A} \begin{bmatrix} y_{21} & 0 & x_{12} \\ 0 & x_{12} & y_{21} \\ y_{32} & 0 & x_{23} \\ 0 & x_{23} & y_{32} \\ y_{13} & 0 & x_{31} \\ 0 & x_{31} & y_{13} \end{bmatrix} \begin{bmatrix} E_{11} & E_{12} & E_{13} \\ E_{12} & E_{22} & E_{23} \\ E_{13} & E_{23} & E_{33} \end{bmatrix} \begin{bmatrix} y_{21} & 0 & y_{32} & 0 & y_{13} & 0 \\ 0 & x_{12} & 0 & x_{23} & 0 & x_{31} \\ x_{12} & y_{21} & x_{23} & y_{32} & x_{31} & y_{13} \end{bmatrix}. \quad (15.46)$$

The computation of consistent body forces is left as an Exercise.

```

Trig3VeubekeMembraneStiffness[ncoor_,Emat_,h_,numer_]:=Module[{
  x1,x2,x3,y1,y2,y3,x12,x23,x31,y21,y32,y13,A,Be,Te,Ke},
  {{x1,y1},{x2,y2},{x3,y3}}=ncoor;
  A=Simplify[(x2*y3-x3*y2+(x3*y1-x1*y3)+(x1*y2-x2*y1))/2];
  {x12,x23,x31,y21,y32,y13}={x1-x2,x2-x3,x3-x1,y2-y1,y3-y2,y1-y3};
  Be={{y21,0,y32,0,y13,0},{0,x12,0,x23,0,x31},
      {x12,y21,x23,y32,x31,y13}}/A;
  If[numer,Be=N[Be]]; Ke=A*h*Transpose[Be].Emat.Be;
  Return[Ke]];

```

FIGURE 15.12. Implementation of Veubeke equilibrium triangle stiffness matrix as a *Mathematica* module.

§15.5.3. *Implementation

The implementation of the Veubeke equilibrium triangle as a *Mathematica* module that returns \mathbf{K}^e is shown in Figure 15.12. It needs only 8 lines of code. It is invoked as

$$\mathbf{K}^e = \text{Trig3VeubekeMembraneStiffness}[\text{ncoor}, \text{Emat}, h, \text{numer}]; \quad (15.47)$$

The arguments have the same meaning as those of the module `Trig3TurnerMembraneStiffness` described in §15.3.6.

```

ncoor={{0,0},{3,1},{2,2}}; Emat=8*{{8,2,0},{2,8,0},{0,0,3}};
Ke=Trig3VeubekeMembraneStiffness[ncoor,Emat,1,False];
Print["Ke=",Ke//MatrixForm];
Print["eigs of Ke=",Chop[Eigenvalues[N[Ke]]]];

```

$$\mathbf{K}^e = \begin{pmatrix} 140 & -60 & -4 & -28 & -136 & 88 \\ -60 & 300 & -12 & -84 & 72 & -216 \\ -4 & -12 & 44 & 20 & -40 & -8 \\ -28 & -84 & 20 & 44 & 8 & 40 \\ -136 & 72 & -40 & 8 & 176 & -80 \\ 88 & -216 & -8 & 40 & -80 & 176 \end{pmatrix}$$

$$\text{eigs of } \mathbf{K}^e = \{557.318, 240., 82.6816, 0, 0, 0\}$$

FIGURE 15.13. Test statements to exercise the module of Figure 15.12, and outputs.

This module is exercised by the statements listed at the top of Figure 15.13, which form a triangle with corner coordinates $\{(0,0), (3,1), (2,2)\}$, isotropic material matrix with $E_{11} = E_{22} = 64$, $E_{12} = 16$, $E_{33} = 24$, others zero, and unit thickness. The results are shown at the bottom of Figure 15.13. This is the same triangle used to test module `Trig3TurnerMembraneStiffness` in §15.3.6. Note that the element is rank sufficient.

§15.5.4. *Spurious Kinematic Modes

Although an individual Veubeke equilibrium triangle is rank sufficient, assemblies are prone to the appearance of spurious mechanisms. That is, kinematic modes that produce no strain energy although they are not rigid body modes. These will be illustrated by studying the three macroelements pictured in Figure 15.14. For simplicity the macroelements are of rectangular shape, but the conclusions apply to more general geometries.

Type I macroelement is built with two triangles. It has four geometric nodes: 1–4, five connection nodes: 5–9, and 10 degrees of freedom. The eigenvalue analysis of the assembled stiffness \mathbf{K} is given as an Exercise. It shows that \mathbf{K} has 4 zero eigenvalues. Since there are 3 rigid body modes in 2D, one is spurious. It is easily

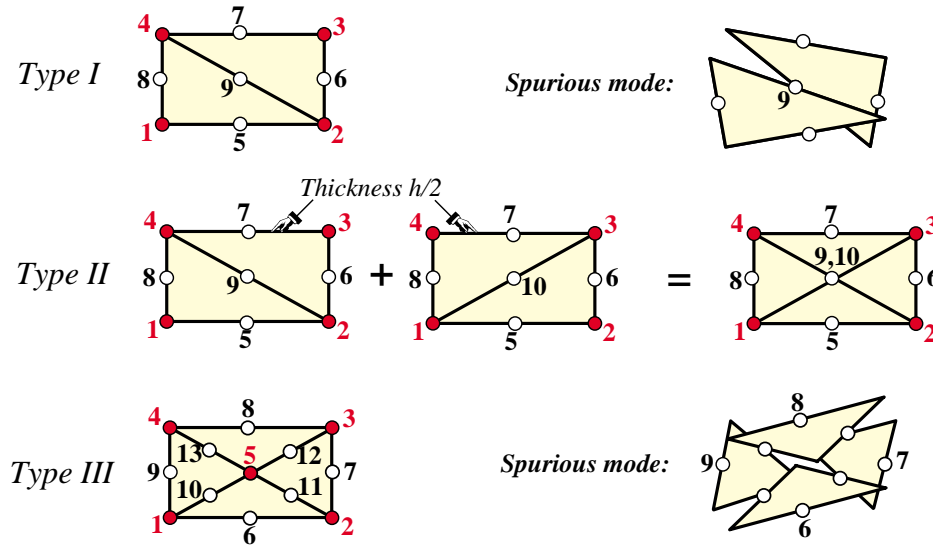


FIGURE 15.14. Three macroelement assemblies fabricated with Veubeke equilibrium triangles to investigate spurious kinematic modes. Red-filled and white-filled circles mark geometric and connection nodes, respectively.

shown that the spurious mode corresponds to the relative rotation of the two triangles with center node 9 as pivot, as pictured to the right of the macroelement.

Type II macroelement is built with four crisscrossed triangles of thickness $h/2$ as illustrated in the Figure. It has four geometric nodes: 1–4, six connection nodes: 5–10, and 12 degrees of freedom. (Note that although 9 and 10 occupy the same location for this geometry, they should be considered as two separate nodes.) The eigenvalue analysis of the assembled stiffness \mathbf{K} is given as an Exercise. It shows that \mathbf{K} has 3 zero eigenvalues and therefore this macroelement has no spurious modes.

Type III macroelement is of Union-Jack type and is built with 4 triangles. It has five geometric nodes: 1–5, eight connection nodes: 6–13, and 16 degrees of freedom. The eigenvalue analysis of the assembled stiffness \mathbf{K} is given as an Exercise. It shows that \mathbf{K} has 4 zero eigenvalues and consequently one spurious mode. This correspond to the triangles rotating about the midpoints 6–9 as pivots, as pictured to the right of the macroelement.

These examples show that this element, when used in a stiffness code, is prone to *spurious pivot modes* where sides of adjacent triangles rotate relatively from each other about the midpoint connector. This is a consequence of the element being nonconforming: full determination of linearly varying side displacements requires two nodes over that side, and there is only one. Even if a rank sufficiently macroelement mesh unit such as Type II of Figure 15.14 can be constructed, there is no guarantee that spurious pivot modes will not occur when those mesh units are connected. For this reason this element is rarely used in DSM-based structural programs, but acquires importance in applications where flux conservation is important.

§15.6. *Shear Locking in Turner Triangles

A well known deficiency of the 3-node Turner triangle is inability to follow rapidly varying stress fields. This is understandable since stresses within the element, for uniform material properties, are constant. But its 1D counterpart: the 2-node bar element, is nodally exact for displacements under some mild assumptions stated in Chapter 11, and correctly solves loaded-at-joints trusses with one element per member. On the other hand, the triangle can be *arbitrarily way off* under unhappy combinations of loads, geometry and meshing.

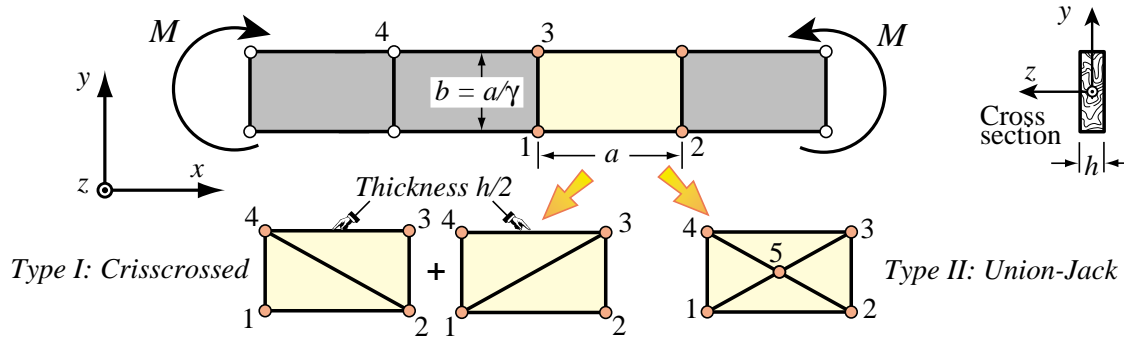


FIGURE 15.15. The bending test with two macroelement types.

What happens in going from 1D to 2D? New effects emerge, notably shear energy and inplane bending. These two can combine to produce *shear locking*: elongated triangles can become extraordinarily stiff under inplane bending because of *spurious shear energy*.⁶ The bad news for engineers is that wrong answers caused by locking are *non-conservative*: deflections and stresses can be so grossly underestimated that safety margins are overwhelmed.

To characterize shear locking quantitatively it is convenient to use macroelements in which triangles are combined to form a 4-node rectangle. This simplifies repetition to form regular meshes. The rectangle response under in-plane bending is compared to that of a Bernoulli-Euler beam segment. It is well known that the latter is exact under constant moment. The response ratio of macroelement to beam is a good measure of triangle performance under bending. Such benchmarks are technically called *higher order patch tests*. Test results can be summarized by one number: the *energy ratio*, which gives a scalar measure of relative stiffness.

§15.6.1. *The Inplane Bending Test

The test is defined in Figure 15.15. A Bernoulli-Euler plane beam of thin rectangular cross-section of height b and thickness h is bent under applied end moments M . The beam is fabricated of isotropic material with elastic modulus E and Poisson's ratio ν . Except for possible end effects the exact solution of the beam problem (from both the theory-of-elasticity and beam-theory standpoints) is a constant bending moment $M(x) = M$ along the span. The associated curvature is $\kappa = M/(EI_{zz}) = 12M/(Eb^3h)$. The exact energy taken by a beam segment of length a is $U_{\text{beam}} = \frac{1}{2}M\kappa a = \frac{6M^2 a}{Eb^3h} = \frac{1}{24}Eb^3h\kappa^2 a = \frac{1}{24}Eb^3h\theta_a^2/a$. In the latter $\theta_a = \kappa a$ is the relative rotation of two cross sections separated by a .

To study the bending performance of triangles the beam is modeled with one layer of identical rectangular macroelements dimensioned $a \times b$ and made up of triangles, as illustrated in Figure 15.15. The rectangle aspect ratio is $\gamma = a/b$. All rectangles undergo the same deformations and thus it is enough to study a individual macroelement 1-2-3-4. Two types are considered here:

Crisscrossed (CC). Formed by overlaying triangles 1-2-4, 3-4-2, 2-3-1 and 4-1-2, each with thickness $h/2$. Using 4 triangles instead of 2 makes the macroelement geometrically and physically symmetric since 2 triangles are attached to each corner.

Union-Jack (UJ). Formed by placing a fifth node at the center and dividing the rectangle into 4 triangles: 1-2-5, 2-3-5, 3-4-5, 4-1-5. By construction this element is also geometrically and physically symmetric.

⁶ The deterioration can be even more pronounced for its spatial counterpart: the 4-node tetrahedron element, because shear effects are even more important in three dimensions.

§15.6.2. *Energy Ratios

The assembled macroelement stiffnesses are \mathbf{K}_{CC} and \mathbf{K}_{UJ}^+ , of orders 8×8 and 10×10 , respectively. For the latter the internal node 5 is statically condensed producing an 8×8 stiffness \mathbf{K}_U . To test performance we apply four alternating corner loads as shown in Figure 15.16. The resultant bending moment is $M = Pb$.

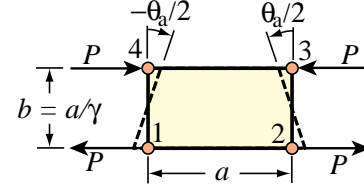


FIGURE 15.16. Bending a macroelement by applying a relative edge rotation.

Although triangles cannot copy curvatures pointwise,⁷ macroelement edges can rotate since constituent triangles can expand or contract. Because of symmetries, the rotations of sides 1-2 and 3-4 are $-\theta_a/2$ and $\theta_a/2$, as illustrated in Figure 15.16. The corresponding corner x displacements are $\pm b\theta_a/4$ whereas the y displacements are zero. Assemble these into a node displacement 8-vector \mathbf{u}_M .

$$\mathbf{u}_M = \frac{1}{4}b\theta_a [-1 \ 0 \ 1 \ 0 \ -1 \ 0 \ 1 \ 0]^T \quad (15.48)$$

The internal energy taken by a macroelement of 8×8 stiffness \mathbf{K}_M under (15.48) is $U_M = \frac{1}{2}\mathbf{u}_M^T \mathbf{K}_M \mathbf{u}_M$, which can be expressed as a function of E , ν , a , b , h and θ_a .⁸

```
ClearAll[a,b,Em,h,γ];
b=a/γ; Iz=h*b^3/12; Ubeam=Simplify[(1/2)*Em*Iz*θa^2/a];
Emat=Em*{{1,0,0},{0,1,0},{0,0,1/2}};
nc={{-a,-b},{a,-b},{a,b},{-a,b},{0,0}}/2;
enCC={{1,2,4},{3,4,2},{2,3,1},{4,1,3}};
enUJ={{1,2,5},{2,3,5},{3,4,5},{4,1,5}}; r={0,0};
For [m=1,m<=2,m++, mtype={"CC","UJ"}[[m]];
  nF={8,10}[[m]]; K=Table[0,{nF},{nF}]; f=Table[0,{nF}];
  For [e=1,e<=4,e++,
    If [mtype=="CC", enl=enCC[[e]], enl=enUJ[[e]]];
    {n1,n2,n3}=enl; encoor={nc[[n1]],nc[[n2]],nc[[n3]]];
    ht=h; If [mtype=="CC", ht=h/2];
    Ke=Trig3TurnerMembraneStiffness[enCoor,Emat,ht,False];
    eft={2*n1-1,2*n1,2*n2-1,2*n2,2*n3-1,2*n3};
    For [i=1,i<=6,i++, For [j=1,j<=6,j++, ii=eft[[i]];
      jj=eft[[j]]; K[[ii,jj]]+=Ke[[i,j]] ];
    ]; KM=K=Simplify[K];
    If [mtype=="UJ",
      {K,f}=Simplify[CondenseLastFreedom[K,f]];
      {KM,f}=Simplify[CondenseLastFreedom[K,f]];
    Print["KM=",KM/MatrixForm];
    uM={1,0,-1,0,1,0,-1,0}*θa*b/4;
    UM=uM.KM.uM/2; rM=Simplify[UM/Ubeam];
    Print["rM=",rM]; r[[m]]=rM;
  ];
Plot[Evaluate[r],{γ,0,10}];
```

FIGURE 15.17. Script to compute energy ratios for the two macroelements of Figure 15.15.

The ratio $r_M = U_M/U_{beam}$ is called the *energy ratio*. If $r_M > 1$ the macroelement is stiffer than the beam because it takes more energy to bend it to conform to the same edge rotations, and the 2D model is said to be *overstiff*. Results for zero Poisson's ratio, computed with the script of Figure 15.17, are

$$r_{CC} = 3 + \frac{3}{2}\gamma^2, \quad r_{UJ} = \frac{3(1+\gamma^2)^2}{2+4\gamma^2}. \quad (15.49)$$

⁷ That is the reason why they can be so stiff under bending.

⁸ The load P could be recovered via $\mathbf{K}_M \mathbf{u}_M$, but this value is not needed to compute energy ratios.

If for example $\gamma = a/b = 10$, which is an elongated rectangular shape of 10:1 aspect ratio, $r_{CC} = 153$ and the crisscrossed macroelement is 153 times stiffer than the beam. For the Union-Jack configuration $r_{UJ} = 10201/134 = 76.13$; about twice better but still way over stiff. If $\gamma = 1$, $r_{CC} = 4.5$ and $r_{UJ} = 2$: over stiff but not dramatically so. The effect of a nonzero Poisson's ratio is studied in Exercise 15.10.

§15.6.3. *Convergence as Mesh is Refined

Note that if $\gamma = a/b \rightarrow 0$, $r_{CC} \rightarrow 3$ and $r_{UJ} \rightarrow 1.5$. So even if the beam of Figure 15.15 is divided into an infinite number of macroelements along x the solution will not converge. It is necessary to subdivide also along the height. If $2n$ ($n \geq 1$) identical macroelement layers are placed along the beam height while γ is kept fixed, the energy ratio becomes

$$r^{(2n)} = \frac{2^{2n} - 1 + r^{(1)}}{2^{2n}} = 1 + \frac{r^{(1)} - 1}{2^{2n}}, \quad (15.50)$$

where $r^{(1)}$ is the ratio (15.49) for one layer. If $r^{(1)} = 1$, $r^{(2n)} = 1$ for all $n \geq 1$, so bending exactness is maintained as expected. If $n = 1$ (two layers), $r^{(2)} = (3 + r^{(1)})/4$ and if $n = 2$ (four layers), $r^{(4)} = (7 + r^{(1)})/8$.

If $n \rightarrow \infty$, $r^{(2n)} \rightarrow 1$, but convergence can be slow. For example, suppose that $\gamma = 1$ (unit aspect ratio $a = b$) and that $r^{(1)} = r_{CC} = 4.5$. To get within 1% of the exact solution, $1 + 3.5/2^{2n} < 1.01$. This is satisfied if $n \geq 5$, meaning 10 layers of elements along y . If the beam span is 10 times the height, 1000 macroelements or 4000 triangles are needed for this simple problem, which is exactly solvable by one beam element.

The stress accuracy of triangles is examined in Chapter 28.

Notes and Bibliography

As a plane stress structural element, the Turner triangle was first developed in the 1956 paper by Turner et. al. [254]. The target application was modeling of delta wing skin panels. Arbitrary quadrilaterals were formed by assembling triangles as macroelements. Because of its geometric flexibility, the element was soon adopted in aircraft structural analysis codes in the late 1950's. It moved to Civil Engineering applications through the research and teaching at Berkeley of Ray Clough, who gave the method its name in [39].

The derivation method of [254] would look unfamiliar to present FEM practitioners used to the displacement method. It was based on assumed stress modes. More precisely: the element, referred to a local Cartesian system $\{x, y\}$, is put under three constant stress states: σ_{xx} , σ_{yy} and σ_{xy} , collected in array σ . Lumping the stress field to the nodes gives the node forces: $\mathbf{f} = \mathbf{L}\sigma$. The strain field computed from stresses is $\mathbf{e} = \mathbf{E}^{-1}\sigma$. This is integrated to get a deformation-displacement field, to which 3 rigid-body modes are added as integration constants. Evaluating at the nodes produces $\mathbf{e} = \mathbf{A}\mathbf{u}$, and the stiffness matrix follows on eliminating σ and \mathbf{e} : $\mathbf{K} = \mathbf{L}\mathbf{E}\mathbf{A}$. For constant thickness and material properties it happens that $\mathbf{L} = \mathbf{V}\mathbf{A}^T$ and so $\mathbf{K} = \mathbf{V}\mathbf{A}^T\mathbf{E}\mathbf{A}$ happily turned out to be symmetric. This \mathbf{A} is the \mathbf{B} of (15.17) times $2A$, so in the end the stiffness matrix (for constant plate thickness) turns out to be the same as (15.21).

The derivation from assumed displacements evolved later. It is not clear who worked it out first, although it is mentioned in [39,267]. The equivalence of the two forms, through energy principles, had been noted by Gallagher [107]. Early displacement derivations typically started from linear polynomials in Cartesian coordinates. For example Przemieniecki [204] begins with

$$u_x = c_1x + c_2y + c_3, \quad u_y = c_4x + c_5y + c_6. \quad (15.51)$$

Here the c_i play the role of generalized coordinates, which have to be eventually eliminated in favor of node displacements. The same approach is used by Clough in a widely disseminated 1965 article [41]. Even for this simple element the approach is unnecessarily complicated and leads to long hand computations. The elegant derivation in triangular coordinates was popularized by Argyris [10].

The idea of using piecewise linear interpolation over a triangular mesh actually precedes [254] by 13 years. As noted in Chapter 1, it appears in an article by Courant [54], where it is applied to a Poisson’s equation modeling St. Venant’s torsion. The idea did not influence early work in FEM, however, since as noted above the derivation in [254] was not based on displacement interpolation.

The Veubeke equilibrium triangle appears in [100, p. 170] and is further elaborated in [101, p. 176]. It is constructed there as an *equilibrium element*, that is, the stress field inside the triangle is assumed to be $\sigma_{xx} = \beta_1$, $\sigma_{yy} = \beta_2$ and $\sigma_{xy} = \beta_3$, where $\{\beta_1, \beta_2, \beta_3\}$ are stress parameters. (A field of constant stresses satisfies identically the plane-stress differential equilibrium equations for zero body forces.) Stress parameters can be uniquely expressed in terms of generalized edge loads, which turn out to be virtual-work conjugate to midside displacements.⁹ The direct displacement derivation given here as a “Turner triangle mapping” is new. As previously noted, this element is rarely used in structural mechanics because of the danger of spurious kinematic modes discussed in §15.5.4. It has importance, however, in some non-structural applications.

The completeness check worked out in §15.4.2 is a specialization case of a general proof developed by Irons in the mid 1960s (see [147, §3.9] and references therein) for general isoparametric elements. The check works because the Turner triangle *is* isoparametric.

What are here called triangular coordinates were introduced by Möbius in his 1827 book [183].¹⁰ They are often called barycentric coordinates on account on the interpretation discussed in [55]. Other names are listed in Table 15.1. Triangles possess many fascinating geometric properties studied even before Euclid. An exhaustive development can be found, in the form of solved exercises, in [222].

It is unclear when the monomial integration formula (15.26) was first derived. As an expression for integrands expressed in triangular coordinates it was first stated in [67].

The natural strain derivation of §15.4 is patterned after that developed for the so-called ANDES (Assumed Natural Deviatoric Strain) elements [182]. For the Turner triangle it provides nothing new aside of fancy terminology. Energy ratios of the form used in §15.6 were introduced in [28] as a way to tune up the stiffness of Free-Formulation elements.

References

Referenced items have been moved to Appendix R.

⁹ The initial step of assuming stresses exactly mimics that of [254] a decade earlier. What is fundamentally different in Fraeijs de Veubeke’s derivation is the use of energy theorems (in this case, PVW) to pass from generalized edge loads to mean edge displacements. The approach is characteristic of FEM Generation 2.

¹⁰ He is better remembered for the “Möbius strip” or “Möbius band,” the first one-sided 3D surface in mathematics.

Homework Exercises for Chapter 15

The Linear Plane Stress Triangle

EXERCISE 15.1 [A:15] Assume that the 3-node plane stress triangle has *variable* thickness defined over the element by the linear interpolation formula

$$h(\zeta_1, \zeta_2, \zeta_3) = h_1\zeta_1 + h_2\zeta_2 + h_3\zeta_3, \quad (\text{E15.1})$$

where h_1 , h_2 and h_3 are the thicknesses at the corner nodes. Show that the element stiffness matrix is still given by (15.21) but with h replaced by the mean thickness $h_m = (h_1 + h_2 + h_3)/3$. *Hint*: use (15.20) and (15.26).

EXERCISE 15.2 [A:20] The exact integrals of triangle-coordinate monomials over a straight-sided triangle are given by the formula (15.26), where A denotes the area of the triangle, and i , j and k are nonnegative integers. Tabulate the right-hand side for combinations of exponents i , j and k such that $i + j + k \leq 3$, beginning with $i = j = k = 0$. Remember that $0! = 1$. (*Labor-saving hint*: don't bother repeating exponent permutations; for example $i = 2, j = 1, k = 0$ and $i = 1, j = 2, k = 0$ are permutations of the same thing. Hence one needs to tabulate only cases in which $i \geq j \geq k$).

EXERCISE 15.3 [A/C:20] Compute the consistent node force vector \mathbf{f}^e for body loads over a Turner triangle, if the element thickness varies as per (E15.1), $b_x = 0$, and $b_y = b_{y1}\zeta_1 + b_{y2}\zeta_2 + b_{y3}\zeta_3$. Check that for $h_1 = h_2 = h_3 = h$ and $b_{y1} = b_{y2} = b_{y3} = b_y$ you recover (15.25). For area integrals use (15.26). Partial result: $f_{y1} = (A/60)[b_{y1}(6h_1 + 2h_2 + 2h_3) + b_{y2}(2h_1 + 2h_2 + h_3) + b_{y3}(2h_1 + h_2 + 2h_3)]$.

EXERCISE 15.4 [A/C:20] Derive the formula for the consistent force vector \mathbf{f}^e of a Turner triangle of constant thickness h , if side 1-2 ($\zeta_3 = 0, \zeta_2 = 1 - \zeta_1$), is subject to a linearly varying boundary force $\mathbf{q} = h\hat{\mathbf{t}}$ such that

$$\begin{aligned} q_x &= q_{x1}\zeta_1 + q_{x2}\zeta_2 = q_{x1}(1 - \zeta_2) + q_{x2}\zeta_2, \\ q_y &= q_{y1}\zeta_1 + q_{y2}\zeta_2 = q_{y1}(1 - \zeta_2) + q_{y2}\zeta_2. \end{aligned} \quad (\text{E15.2})$$

This “line boundary force” \mathbf{q} has dimension of force per unit of side length.

Procedural Hint. Use the last term of the line integral (14.21), in which $\hat{\mathbf{t}}$ is replaced by \mathbf{q}/h , and show that since the contribution of sides 2-3 and 3-1 to the line integral vanish,

$$W^e = (\mathbf{u}^e)^T \mathbf{f}^e = \int_{\Gamma^e} \mathbf{u}^T \mathbf{q} d\Gamma^e = \int_0^1 \mathbf{u}^T \mathbf{q} L_{21} d\zeta_2, \quad (\text{E15.3})$$

where L_{21} is the length of side 1-2. Replace $u_x(\zeta_2) = u_{x1}(1 - \zeta_2) + u_{x2}\zeta_2$; likewise for u_y , q_x and q_y , integrate and identify with the inner product shown as the second term in (E15.3). Partial result: $f_{x1} = L_{21}(2q_{x1} + q_{x2})/6$, $f_{x3} = f_{y3} = 0$.

Note. The following *Mathematica* script solves this Exercise. If you decide to use it, explain the logic.

```
ClearAll[ux1, uy1, ux2, uy2, ux3, uy3, z2, L12];
ux=ux1*(1-z2)+ux2*z2; uy=uy1*(1-z2)+uy2*z2;
qx=qx1*(1-z2)+qx2*z2; qy=qy1*(1-z2)+qy2*z2;
We=Simplify[L12*Integrate[qx*ux+qy*uy, {z2, 0, 1}]];
fe=Table[Coefficient[We, {ux1, uy1, ux2, uy2, ux3, uy3}][[i]], {i, 1, 6}];
fe=Simplify[fe]; Print["fe=", fe];
```

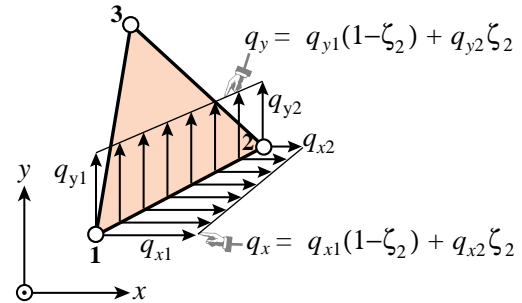


FIGURE E15.1. Line force on triangle side 1-2 for Exercise 15.4.

EXERCISE 15.5 [C+N:15] Compute the entries of \mathbf{K}^e for the following plane stress triangle:

$$x_1 = 0, y_1 = 0, x_2 = 3, y_2 = 1, x_3 = 2, y_3 = 2, \quad (E15.4)$$

$$\mathbf{E} = \begin{bmatrix} 100 & 25 & 0 \\ 25 & 100 & 0 \\ 0 & 0 & 50 \end{bmatrix}, \quad h = 1.$$

This may be done by hand (it is a good exercise in matrix multiplication) or (more quickly) using the script of Figure 15.5. Partial result: $K_{11} = 18.75$, $K_{66} = 118.75$.

EXERCISE 15.6 [A+C:15] Show that the sum of the rows (and columns) 1, 3 and 5 of \mathbf{K}^e as well as the sum of rows (and columns) 2, 4 and 6 must vanish, and explain why. Check it with the foregoing script.

EXERCISE 15.7 [A:10]. Consider two triangles T and T^* , both with positive area. The corner coordinates of T are $\{\{x_1, y_1\}, \{x_2, y_2\}, \{x_3, y_3\}\}$ and those of T^* are $\{\{x_1^*, y_1^*\}, \{x_2^*, y_2^*\}, \{x_3^*, y_3^*\}\}$. A point P in T has Cartesian coordinates $\{x, y\}$ and triangular coordinates $\{\zeta_1, \zeta_2, \zeta_3\}$. A point P^* in T^* has Cartesian coordinates $\{x^*, y^*\}$ and the same triangular coordinates. Show that $\{x^*, y^*\}$ and $\{x, y\}$ are connected by the affine transformation

$$\begin{bmatrix} 1 \\ x^* \\ y^* \end{bmatrix} = \begin{bmatrix} 1 & 1 & 1 \\ x_1^* & x_2^* & x_3^* \\ y_1^* & y_2^* & y_3^* \end{bmatrix} \begin{bmatrix} 1 & 1 & 1 \\ x_1 & x_2 & x_3 \\ y_1 & y_2 & y_3 \end{bmatrix}^{-1} \begin{bmatrix} 1 \\ x \\ y \end{bmatrix} \quad (E15.5)$$

(The indicated inverse exists if T has positive area, as assumed.)

EXERCISE 15.8 [A:15]. Let point P have triangular coordinates $\{\zeta_1^P, \zeta_2^P, \zeta_3^P\}$, as shown in Figure E15.2. Find the distances h_{P1} , h_{P2} and h_{P3} of P to the three triangle sides, and the triangular coordinates of points P_1 , P_2 and P_3 shown in the Figure (P_i is projection on the side opposite to corner i .) Show that $h_{Pi} = \zeta_{Pi} h_i = 2\zeta_{Pi} A/L_{kj}$, for $i = 1, 2, 3$, $j = 2, 3, 1$ and $k = 3, 1, 2$, in which L_{ji} denotes the length of the side that joins corners i and j and h_i is the distance from corner i to the opposite side, as illustrated in Figure E15.2. (Note: the distances $\{h_{P1}, h_{P2}, h_{P3}\}$ are called the *trilinear coordinates* of a point P with respect to the vertices of the triangle. They were introduced by Plücker in 1835. They are essentially scaled versions of the triangular coordinates.)

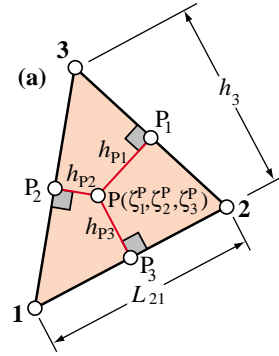


FIGURE E15.2. Distances of arbitrary point P to three triangle sides.

EXERCISE 15.9 [A:10]. Express the distances from the triangle centroid to the 3 sides in term of the triangle area and the side lengths. Answer: $\frac{2}{3}A/L_{21}$, $\frac{2}{3}A/L_{32}$ and $\frac{2}{3}A/L_{13}$, where A is the area of the triangle assumed positive and L_{ji} is the length of side that joins corners i and j , cf. Figure E15.2, Hint: the area of each subtriangle subtended by the centroid and two corners is $\frac{1}{3}A$.

EXERCISE 15.10 [A:20] Find the triangular coordinates of the altitude feet points H_1 , H_2 and H_3 pictured in Figure 15.3. Once these are obtained, find the equations of the altitudes in triangular coordinates, and the coordinates of the orthocenter H . Answer for H_3 : $\zeta_1 = \frac{1}{2} + (L_{13}^2 - L_{32}^2)/(2L_{21}^2)$, where L_{ji} is the length of side that joins corners i and j ; cf. Figure E15.2.

EXERCISE 15.11 [C+D:20] Let $p(\zeta_1, \zeta_2, \zeta_3)$ represent a *polynomial* expression in the natural coordinates. The integral

$$\int_{\Omega^e} p(\zeta_1, \zeta_2, \zeta_3) d\Omega \quad (E15.6)$$

over a straight-sided triangle can be computed symbolically by the following *Mathematica* module:

```
IntegrateOverTriangle[expr_, tcoord_, A_, max_] := Module [{p, i, j, k, z1, z2, z3, c, s = 0},
  p = Expand[expr]; {z1, z2, z3} = tcoord;
  For [i = 0, i <= max, i++, For [j = 0, j <= max, j++, For [k = 0, k <= max, k++,
    c = Coefficient[Coefficient[Coefficient[p, z1, i], z2, j], z3, k];
    s += 2*c*(i!*j!*k!)/((i+j+k+2)!);
  ]]];
  Return[Simplify[A*s]] ];
```

This is referenced as `int=IntegrateOverTriangle[p,{z1,z2,z3},A,max]`. Here `p` is the polynomial to be integrated, `z1`, `z2` and `z3` denote the symbols used for the triangular coordinates, `A` is the triangle area and `max` the highest exponent appearing in a triangular coordinate. The module name returns the integral. For example, if `p=16+5*b*z2^2+z1^3+z2*z3*(z2+z3)` the call `int=IntegrateOverTriangle[p,{z1,z2,z3},A,3]` returns `int=A*(97+5*b)/6`. Explain how the module works.

EXERCISE 15.12 [C+D:25] Explain the logic of the script listed in Figure 15.17. Then extend it to account for isotropic material with arbitrary Poisson's ratio ν . Obtain the macroelement energy ratios as functions of γ and ν . Discuss whether the effect of a nonzero ν makes much of a difference if $\gamma \gg 1$.

EXERCISE 15.13 [A/C:25] Verify the conclusions of §15.5.4 as regards rank sufficiency or deficiency of the three Veubeke macroelement assemblies pictured in Figure 15.14. Carry out tests with rectangular macroelements dimensioned $a \times b$, constant thickness h , elastic modulus E and Poisson's ratio 0.

EXERCISE 15.14 [C+D:25] To find whether shear is the guilty party in the poor performance of elongated triangles (as alledged in §15.6) run the script of Figure 15.17 with a zero shear modulus. This can be done by setting `Emat=Em*{{1,0,0},{0,1,0},{0,0,0}}` in the third line. Discuss the result. Can `Em` be subsequently reduced to a smaller (fictitious) value so that $r \equiv 1$ for all aspect ratios γ ? Is this practical?

EXERCISE 15.15 [C+D:25] Access the file `Trig3PlaneStress.nb` from the course Web site by clicking on the appropriate link in Chapter 15 Index. This is a *Mathematica* Notebook that does plane stress FEM analysis using the 3-node Turner triangle.

Download the Notebook into your directory. Load into *Mathematica*. Execute the top 7 input cells (which are actually initialization cells) so the necessary modules are compiled. Each cell is preceded by a short comment cell which outlines the purpose of the modules it holds. Notes: (1) the plot-module cell may take a while to run through its tests; be patient; (2) to get rid of unsightly messages and silly beeps about similar names, initialize each cell twice.

After you are satisfied everything works fine, run the cantilever beam problem, which is defined in the last input cell.

After you get a feel of how this code operate, study the source. Prepare a hierarchical diagram of the modules,¹¹ beginning with the main program of the last cell. Note which calls what, and briefly explain the purpose of

¹¹ A hierarchical diagram is a list of modules and their purposes, with indentation to show dependence, similar to the table of contents of a book. For example, if module AAAA calls BBBB and CCCC, and BBBB calld DDDD, the hierarchical diagram may look like:

```
AAAA - purpose of AAAA
  BBBB - purpose of BBBB
    DDDD - purpose of DDDD
```


each module. Return this diagram as answer to the homework. You do not need to talk about the actual run and results; those will be discussed in Part III.

Hint: a hierarchical diagram for `Trig3PlaneStress.nb` begins like

```
Main program in Cell 8 - drives the FEM analysis
  GenerateNodes - generates node coordinates of regular mesh
  GenerateTriangles - generate element node lists of regular mesh
  .....
```

CCCC - purpose of CCCC